SLAC-PUB-95-7005
September, 1995

Impedance of the PEP-II DIP Screen*

C.-K. Ng
Stanford Linear Accelerator Center
Stanford University, Stanford, CA 94309, USA

and

T. Weiland
University of Technology
FB18, Schlossgartenstr. 8
D64289, Darmstadt, Germany.

Abstract

The vacuum chamber of a storage ring normally consists of periodically spaced pumping slots. The longitudinal impedance of slots are analyzed in this paper. It is found that although the broad-band impedance is tolerable, the narrow-band impedance, as a consequence of the periodicity of the slots, may exceed the stability limit given by natural damping with no feedback system on. Based on this analysis, the PEP-II distributed-ion-pump (DIP) screen uses long grooves with hidden holes cut halfway to reduce both the broad-band and narrow-band impedances.

Presented at the Workshop on Collective Effects and Impedance for B-Factories, Tsukuba, Japan, June 12-17, 1995

*Work supported by Department of Energy, contract DE-AC03-76SF00515.

1 Introduction

For achieving the required pumping speed, the dipole chamber in the High Energy Ring (HER) of the PEP-II B-Factory was designed with periodically spaced pumping slots on one side of the chamber walls [1]. From the standpoint of beam dynamics, the broad-band and narrow-band longitudinal and transverse impedances should be kept to small values to avoid single-bunch and coupled-bunch instabilities. It turns out the longitudinal broad-band impedance is normally small compared with the impedance budget of the ring, while the longitudinal narrow-band impedance due to the periodicity of the slots may exceed the stability limit given by radiation damping with no feedback system on. It is known that hidden slots can reduce both the broad-band and narrow-band impedances by several orders of magnitude [2]. Furthermore, in the PEP-II DIP screen design, hidden holes are used to prevent possible TE radiation into the pump chamber. Thus, the final design of the DIP screen consists of six continuous grooves of 5.64 m long on one side of the dipole chamber walls, and 3 mm holes with spacing 1 mm are cut halfway in the chamber wall along each groove.

The paper is organized as follows. In the next section, a generic vacuum chamber model used in our analysis is described. Section 3 and section 4 calculate the longitudinal broad-band and narrow-band impedances of the slots, respectively. In section 5, the impedance of the PEP-II DIP screen is evaluated. Section 6 gives a summary of our results. It should be pointed out that here only longitudinal impedance is studied. The analysis of the transverse impedance of slots can be found in Ref. [3].

2 Vacuum Chamber Model

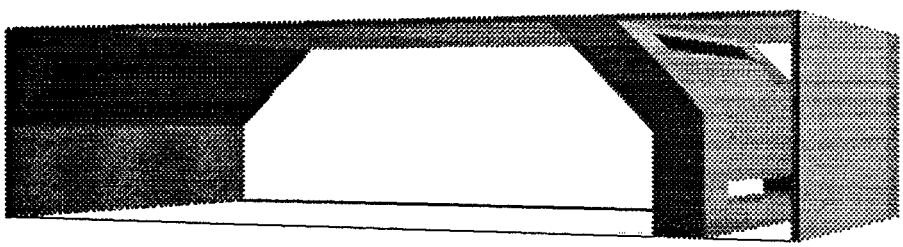

Figure 1: Three dimensional view of a generic vacuum chamber model with four pumping slots connecting the beam chamber with a pump chamber which houses vacuum pumps. For the purpose of impedance analysis the pumps are replaced by a conducting wall. The inner width is 9 cm, the inner height 5 cm, the slot width 3 mm, and the longitudinal slot spacing 1 cm. The only free parameter is the slot length L_{slot} and the number of slotted sections.

Various models of the vacuum chamber have been analyzed for the PEP-II. However, as the basic physical picture is the same for all the different models, only a generic one is considered here. Fig. 1 shows the three-dimensional view of a generic vacuum chamber with slots on one side. The dimensions have been chosen close to the PEP-II design[1],

but may be considered as a generic chamber layout for electron/positron storage rings. Actually, the vacuum chamber of PEP, PETRA and HERA are almost identical in size. All results presented here are per vacuum chamber slotted section and not for the full length of the final chamber. Thus depending on the slot length one has to multiply the single section results with an appropriate factor. For the PEP-II this factor is approximately $1000/L_{slot}(\mathrm{m})$.

3 Longitudinal Broad-band Impedance

The impedance in general depends on the slot length and it saturates when the length is about several times of its width [4]. The pumping requirements are normally set by the total pumping channel cross section. Thus it is worthwhile to investigate the influence of the length of a slot in order to find an optimum slot length from the impedance point of view. The impedance and wake potentials were computed for slot lengths of 2, 3, 4, 5, 10, 20, 40, 80, 160, 320 and 640 mm. As can be seen from Fig. 2, the wake potential converges quite rapidly with the slot length and no significant increase is observed for a slot length greater than 40 mm. Thus long slots are preferable. Furthermore, the wakefield is found to be purely inductive in nature. From the low frequency spectrum of the wakefield, the inductance is determined and its length dependence is shown in Fig. 3. The inductance converges very quickly to a saturated value of 4.0×10^{-5} nH. The loss parameter has similar variation behavior and its saturated value is 7.9×10^{-7} V/pC. This parameter is a good indication of the effective real part of the impedance weighted with the bunch spectrum. The real part of the impedance is obviously rather small compared to the imaginary part. The inductance of all the slots in the ring is approximately 1 nH.

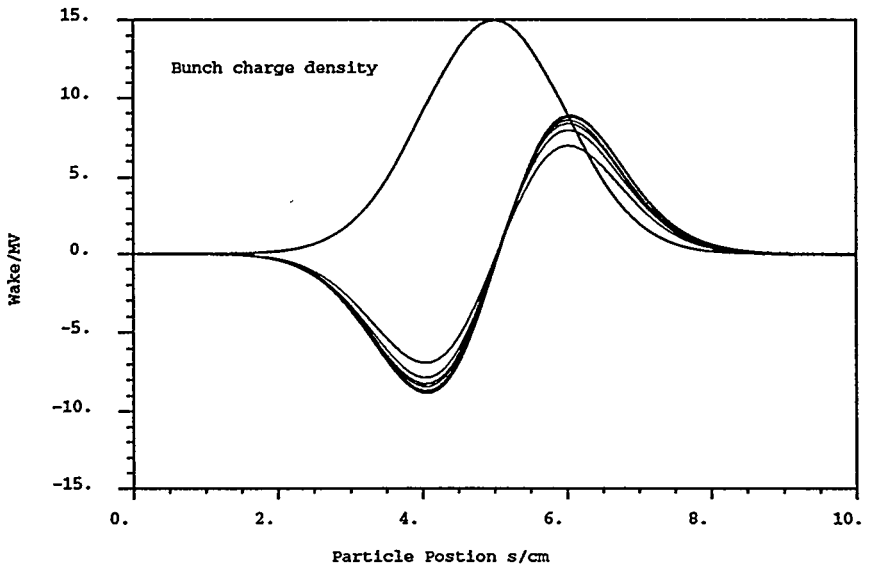

Figure 2: Wake potential as a function of slot length.

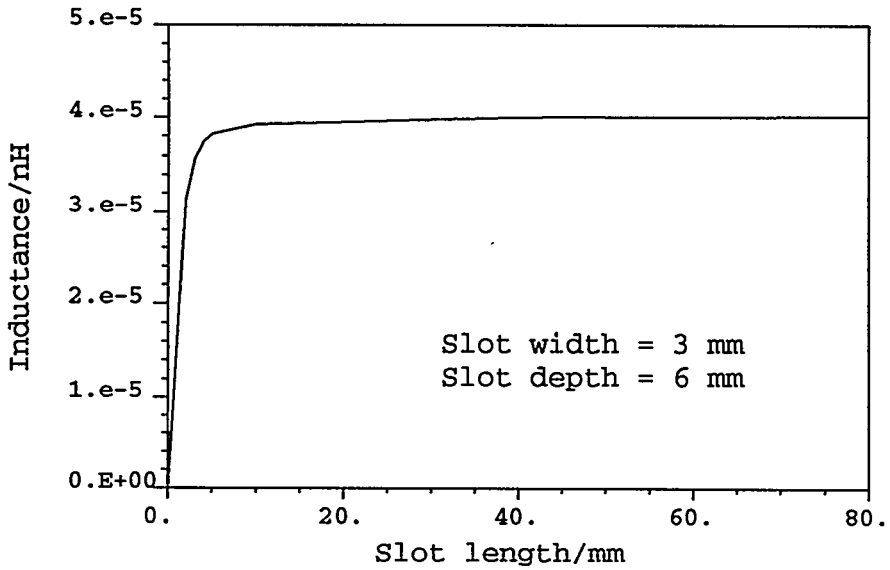

Figure 3: Inductance as a function of slot length.

4 Longitudinal Narrow-band Impedance

Narrow-band impedances are mostly locally confined resonant modes in cavities. A second type of resonant impedance is given by the waveguide character of a vacuum chamber. Basically being a periodic structure, it carries traveling waves with longitudinal and transverse modes just like any traveling wave accelerating structure. There are two possibilities to address this particular impedance, namely frequency and time domain approaches. Strong effects may be found by time domain simulations of a few sections, and weaker effects by modeling the chamber as a periodic structure in frequency domain.

(a) *Section-to-section resonant effects*

In order to identify strong section-to-section effects the wake potentials were computed for pieces consisting of 1,2,4 and 8 sections, with 4 slots per section (see Fig. 1). On the scale where the wake potential is inductive, no significant build-up of a resonant type of impedance has been observed. However, this does not mean that the resonant impedance is negligible but only that it is small compared to the inductive broad-band impedance. Very narrow impedances cannot be found this way but need to be analyzed by frequency domain approaches.

(b) *Traveling Wave Analysis*

As a single mechanical unit, a vacuum chamber is made from 100-200 sections, and an analysis based on infinitely repeating structure is relevant. Thus we can compute traveling waves for any given phase advance per cell. Such a computation results in a Brillouin diagram as one normally finds in linear accelerator designs where similarly long structures (100-200 cavity cells) are used in one unit.

For the vacuum chamber there exist two types of modes. One group shows almost "empty waveguide" mode patterns. A second group shows fields concentrated in the slot

region with almost no field in the center of the vacuum chamber. Examples of these modes for 40 mm slot length are shown in Figs. 4 and 5. In Fig. 6, we show the Brillouin diagram for the structure. The loss parameters, quality factors and shunt impedances for the first seven synchronous waves are listed in Table 2. The mode shown in Fig. 5, a TM_{11}-like mode, has a strong beam coupling. The narrow-band impedance of this mode is about 8 kΩ for the ring, which is roughly a factor of 2 higher than the radiation damping limit at the mode frequency.

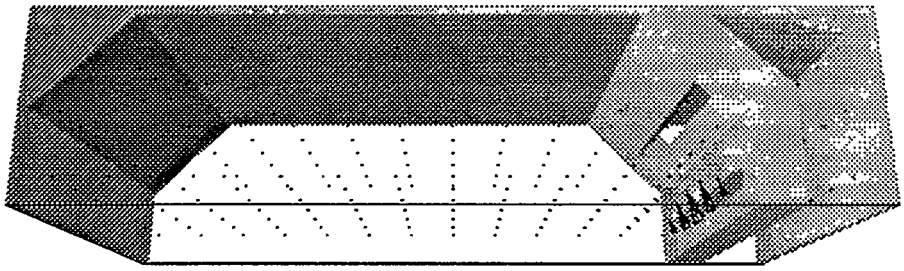

Figure 4: The real part of the electric field of mode 2 with $f = 3.616$ GHz and phase advance 120^o per section.

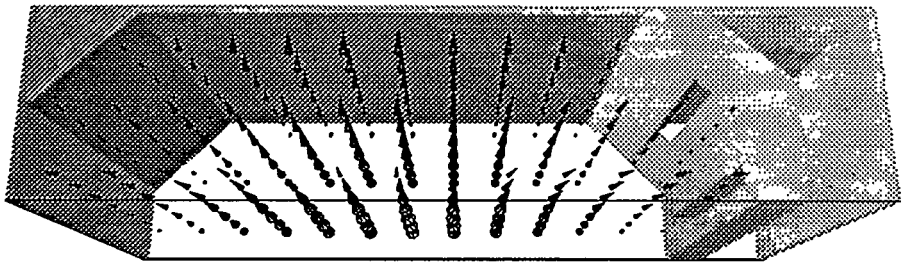

Figure 5: The real part of the electric field of mode 4 with $f = 3.996$ GHz and phase advance 120^o per section.

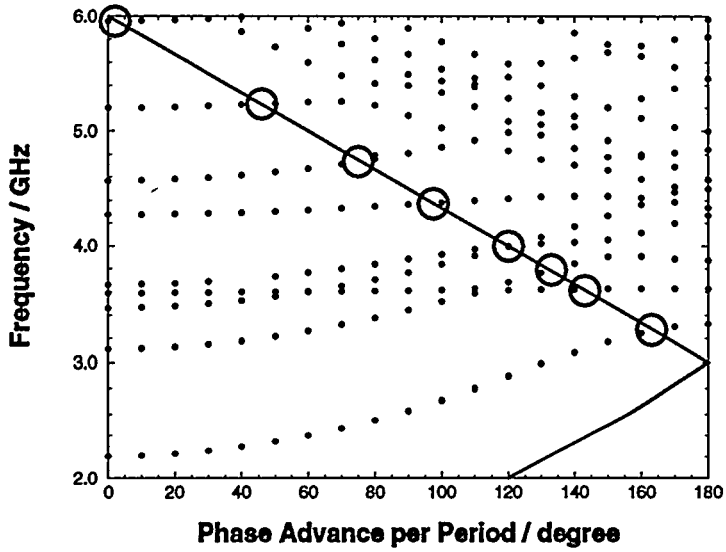

Figure 6: The Brillouin diagram for the vacuum chamber with a slot length of 40 mm and a period of 50 mm. The line light is the solid straight curve. The synchronous modes are marked by circles.

Mode	ϕ /°	f/GHz	k/(V/C)	Q	$R_s/m\Omega$
1	163	3.27	1892	5000	1
2	143	3.63	383	35000	1
3	133	3.80	20170	15000	25
4	120	4.00	148000	27000	318
5	120	4.00	3129	8000	2
6	97	4.37	8129	10000	6
7	75	4.74	23960	37000	60

Table 2. First seven synchronous modes and the associated impedances, quality factors, loss parameters and shunt impedances.

5 PEP-II DIP Screen

From the analysis in the previous two sections, it can be seen that the contribution of the longitudinal broad-band impedance to the total impedance budget of a ring is normally small. The longitudinal narrow-band impedance due to the periodicity of slots may pose problems to coupled-bunched instabilities. The introduction of hidden slots [2] will reduce the broad-band and narrow-band impedances by several orders of magnitude, thus avoiding the complication of randomizing the slots for suppressing the impedance of the resonances excited by the periodic placement of the slots [5].

The final design of the PEP-II DIP screen consists of six continuous grooves of 5.64 m long, 3.75 mm wide and about half the chamber wall thickness located on one side of the dipole chamber walls. Several features of the screen design are in order. First, as seen in section 3, when the length of the groove is greater than a few times of its width, the impedance saturates, and hence the impedance of a 5.64 m long groove along the dipole chamber minimizes the longitudinal broad-band impedance. Second, about half-way deep in the chamber wall, hidden slots are cut along the groove for pumping purposes. Simulations showed that the impedance of a hidden slot is several orders of magnitude smaller than that of a slot of the same length directly cut at the chamber wall. The electromagnetic fields seen by the discontinuities of the hidden slot are suppressed because of the exponential drop-off of the fields into the groove, and consequently the wakefield excitaiton is also reduced exponentially. Third, TE mode traveling waves excited in the ring will radiate into the pump chamber through the slots which may damage the ion pumps. The use of holes instead of slots along the grooves can suppress the TE radiation at the expense of increasing the impedance. In the PEP-II design, 1288 hidden holes each with diameter 3 mm are cut along each groove. Measurements showed that no radiation was observed through the holes [6]. Fourth, the slots are slanted at 45° to protect the distributed ion pumps from single bounce X-rays scattered from the opposite side of the chamber walls.

The impedance of the DIP screen can be separated into two parts: the impedance of the grooves and the impedance of the hidden holes. The impedance of the six grooves

is found to be 1.88×10^{-4} nH. The hidden hole structure is shown in Fig. 7; only half of the structure is modeled because of symmetry. The longitudinal wakefield is shown in Fig. 8, from which the impedance of a column of holes in the six grooves is found to be 4.82×10^{-7} nH. Taking into account of 1288 holes in each groove, the total contribution of all the 192 DIP screens in the HER to the impedance is 0.16 nH, which is less than 1% of the ring impedance budget.

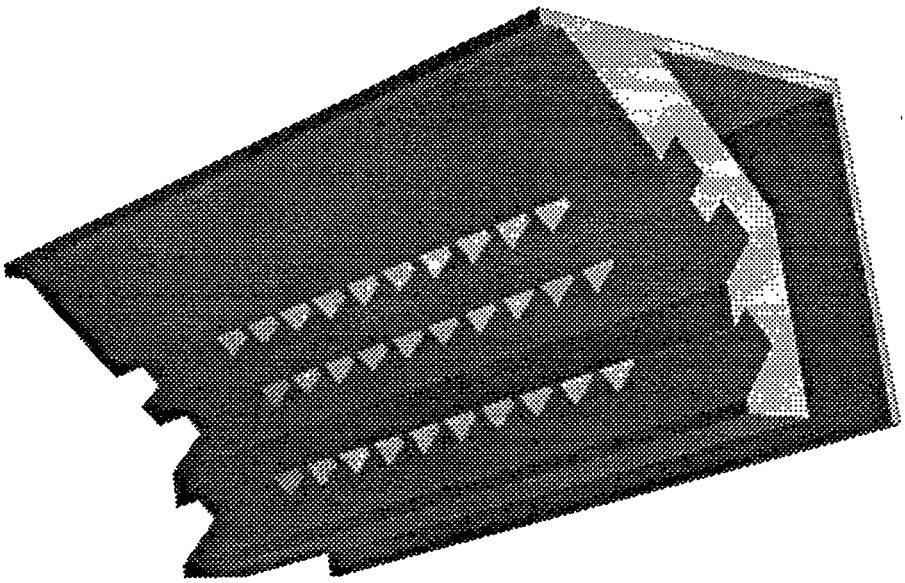

Figure 7: MAFIA model of the PEP-II DIP screen. Ten hidden holes are used in the calculation.

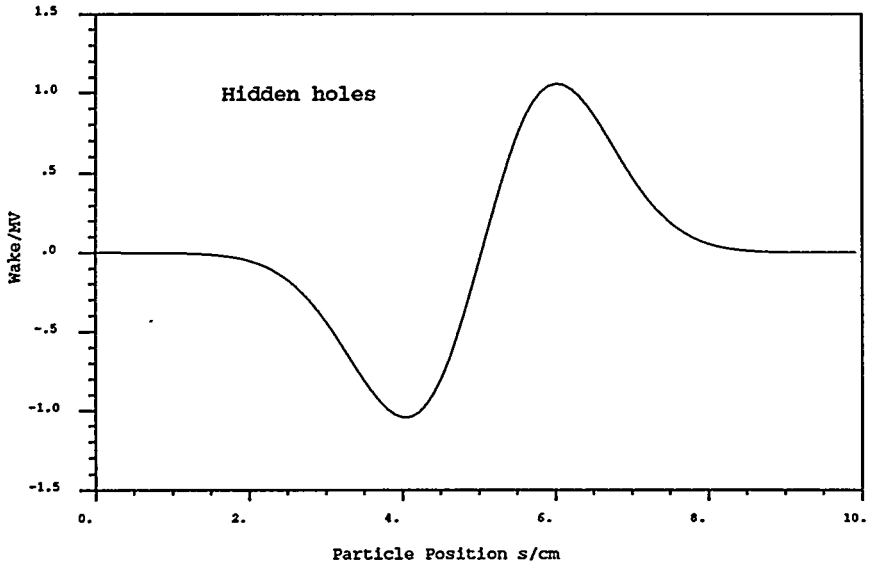

Figure 8: Longitudinal wakefield of the hidden hole structure shown in Fig. 7

6 Summary

The PEP-II DIP screen design uses hidden holes in continuous long grooves which reduces the longitudinal broad-band impedance to very small value, decreases the narrow-band impedance below the limit for coupled-bunch instabilities, and suppresses TE radiation into the pump chambers.

Acknowledgements

We thank A. Chao, E. Daly, S. Heifets, G. Lambertson, M. Nordby and G. Stupakov for useful discussions.

References

[1] An Asymmetric B Factory, Conceptual Design Report, LBL-PUB-5379 or SLAC-418, June 1993.

[2] T. Weiland, Low impedance Vacuum Chambers, PEP-II Technical Note No. 59, 1994.

[3] C.-K. Ng and T. Weiland, Impedance Analysis of the PEP-II Vacuum Chamber, to be published in Proc. of PAC95.

[4] K. L. F. Bane and C.-K. Ng, Impedance Calculations for the Improved SLC Damping Rings, Proc. 1993 PAC, p3432.

[5] G. V. Stupakov, Coupling Impedance of a Long Slot and an Array of Slots in a Circular Vacuum Chamber, SLAC-PUB-6698, 1994.

[6] J. Corlett, private communication.